

Functional reclassification of the putative cinnamyl alcohol dehydrogenase multigene family in *Arabidopsis*

Sung-Jin Kim*, Mi-Ran Kim*, Diana L. Bedgar*, Syed G. A. Moinuddin*, Claudia L. Cardenas*, Laurence B. Davin*, ChulHee Kang[†], and Norman G. Lewis**

*Institute of Biological Chemistry, Washington State University, Pullman, WA 99164-6340; and [†]School of Molecular Biosciences, Washington State University, Pullman, WA 99164-4460

Communicated by Meinhart H. Zenk, Universität Halle, Halle/Saale, Germany, December 2, 2003 (received for review June 23, 2003)

Of 17 genes annotated in the *Arabidopsis* genome database as cinnamyl alcohol dehydrogenase (CAD) homologues, an *in silico* analysis revealed that 8 genes were misannotated. Of the remaining nine, six were catalytically competent for NADPH-dependent reduction of *p*-coumaryl, caffeoyl, coniferyl, 5-hydroxyconiferyl, and sinapyl aldehydes, whereas three displayed very low activity and only at very high substrate concentrations. Of the nine putative CADs, two (AtCAD5 and AtCAD4) had the highest activity and homology ($\approx 83\%$ similarity) relative to bona fide CADs from other species. AtCAD5 used all five substrates effectively, whereas AtCAD4 (of lower overall catalytic capacity) poorly used sinapyl aldehyde; the corresponding 270-fold decrease in k_{enz} resulted from higher K_m and lower k_{cat} values, respectively. No CAD homologue displayed a specific requirement for sinapyl aldehyde, which was in direct contrast with unfounded claims for a so-called sinapyl alcohol dehydrogenase in angiosperms. AtCAD2, 3, as well as AtCAD7 and 8 (highest homology to sinapyl alcohol dehydrogenase) were catalytically less active overall by at least an order of magnitude, due to increased K_m and lower k_{cat} values. Accordingly, alternative and/or bifunctional metabolic roles of these proteins in plant defense cannot be ruled out. Comprehensive analyses of lignified tissues of various *Arabidopsis* knockout mutants (for AtCAD5, 6, and 9) at different stages of growth/development indicated the presence of functionally redundant CAD metabolic networks. Moreover, disruption of AtCAD5 expression had only a small effect on either overall lignin amounts deposited, or on syringyl-guaiacyl compositions, despite being the most catalytically active form *in vitro*.

Cinnamyl alcohol dehydrogenase (CAD), discovered by Zenk and coworkers in 1973 (1, 2), depicts a class of NADPH-dependent enzymes catalyzing reduction of various phenylpropenyl aldehyde derivatives 1–5 (Fig. 1). Generically, this conversion affords monolignols 6–10, with the latter mainly being precursors of lignins and lignans (3–5). Since its discovery, various CAD/CAD homologues were reported as multigene families in many plant species. Yet, despite numerous CAD-like genes being described over nearly 15 years, the paucity of detailed protein biochemical characterization is enigmatic. Frequently, they are arbitrarily assigned roles in monolignols 6–10 and lignin formation (6–13), regardless of, for example, low degree of homology to established CADs, and lack of demonstration of biochemical function *in vitro* and/or physiological role(s).

With the *Arabidopsis* genome completed (14), 17 genes were annotated as CAD homologues (see Table 1 and Table 3, which is published as supporting information on the PNAS web site). Accordingly, with all putative members potentially identified (15), it was possible to comprehensively examine kinetic properties and substrate versatilities *in vitro* as a first step to establishing true physiological function(s) (16, 17).

Initially, *in silico* analysis (18) revealed that only 9 of the 17 genes displayed sufficient homology for consideration as bona fide CADs, six of which are demonstrated herein as being biochemically competent for phenylpropenyl aldehyde 1–5 reduction. These find-

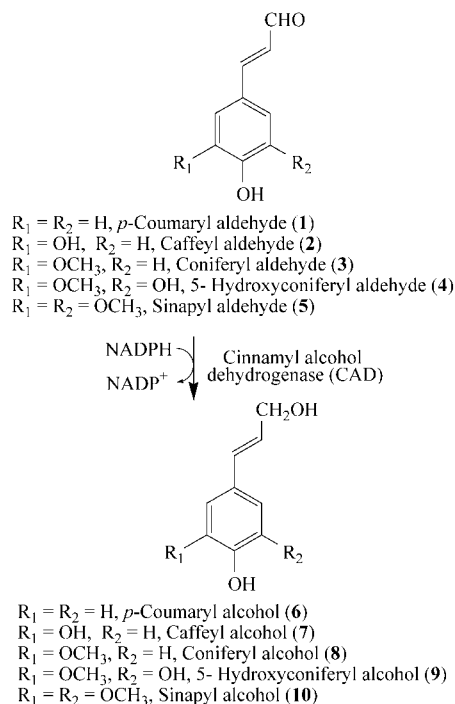


Fig. 1. CAD substrates and products.

ings, together with analysis of selected CAD knockout lines, strongly suggest that lignin, and presumably also lignan, formation are not dependent on a single CAD isoform, due to the presence of functionally redundant, complex metabolic, networks in different tissues, organs, and cell types in *Arabidopsis*. Indeed, the data provide more evidence that CAD does not fulfill a key (rate-limiting) regulatory role in lignin deposition, in contrast to various claims (19) that have consistently lacked supporting scientific data (3). Nor did any homologue display a specific substrate preference [i.e., for sinapyl aldehyde (5) or any other aldehyde] as previously claimed essential for syringyl lignin formation in angiosperms (20). Indeed, genes with closest homology to the so-called sinapyl alcohol dehydrogenase (SAD) isoform displayed the poorest ability to use any of the aldehyde substrates examined, and may instead be

Abbreviations: CAD, cinnamyl alcohol dehydrogenase; SAD, sinapyl alcohol dehydrogenase; S:G, syringyl:guaiacyl.

Data deposition: The sequences reported in this paper have been deposited in the GenBank database [accession nos. AY288079 (AtCAD1), AY302077 (AtCAD2), AY302078 (AtCAD3), AY302081 (AtCAD4), AY302082 (AtCAD5), AY302075 (AtCAD6), AY302079 (AtCAD7), AY302080 (AtCAD8), and AY302076 (AtCAD9)].

[†]To whom correspondence should be addressed. E-mail: lewisn@wsu.edu.

© 2004 by The National Academy of Sciences of the USA

Table 1. Sequence comparisons of an annotated nine-membered CAD multigene family in *Arabidopsis* to bona fide CADs and a putative SAD

Locus no.	Gene annotation	Promoter size, kb	cDNA, kb	Amino acid no.	Mm, kDa	NtCAD, %		PtCAD, %		AsCAD, %		AsSAD, %	
						Similarity	Identity	Similarity	Identity	Similarity	Identity	Similarity	Identity
At4g34230	AtCAD5	1.20	1.07	357	38.7	82.9	76.5	76.5	65.8	82.9	77.9	62.6	53.1
At3g19450	AtCAD4	1.80	1.10	365	39.1	81.5	75.1	74.0	65.8	83.5	78.7	62.5	53.3
At4g37990	AtCAD8	1.72	1.08	359	38.9	63.4	52.7	64.6	53.4	63.8	52.0	78.0	72.1
At2g21730	AtCAD2	2.05	1.13	376	40.9	62.4	51.7	64.7	53.1	64.0	52.7	71.1	62.6
At2g21890	AtCAD3	2.03	1.13	375	40.9	64.0	52.1	64.4	52.8	65.6	53.1	70.2	61.5
At4g37980	AtCAD7	0.60	1.07	357	38.2	61.4	50.1	62.9	52.0	61.4	50.4	77.6	71.4
At4g37970	AtCAD6	0.59	1.09	363	39.0	61.3	51.0	65.5	53.5	62.5	49.3	77.3	68.5
At4g39330	AtCAD9	1.64	1.08	360	38.9	60.2	50.7	63.6	54.1	63.9	53.8	74.4	67.5
At1g72680	AtCAD1	0.40	1.07	355	38.7	57.1	46.0	61.0	47.5	55.1	41.2	58.6	49.3

NtCAD, *Nicotiana tabacum* CAD (GenBank accession no. X62344); PtCAD, *Pinus taeda* CAD (GenBank accession no. Z37992); AsCAD, Aspen CAD (GenBank accession no. AF217957); AsSAD, Aspen SAD (GenBank accession no. AF273256). Mm, molecular mass.

involved in unrelated defense functions. The present study, thus, also underscores the ongoing difficulties arising from arbitrary annotations [in The *Arabidopsis* Information Resource (TAIR) database, which can be accessed at www.arabidopsis.org] of presumed catalytic/physiological functions to various multigene families, such as with CAD, in the *Arabidopsis* genome (18).

Materials and Methods

Plant Materials. Wild-type and T-DNA mutant *Arabidopsis thaliana* plants were grown in Washington State University greenhouses.

Materials, Instrumentation, and Chemical Syntheses. For more information, see *Supporting Methods*, which is published as supporting information on the PNAS web site.

CAD Homologues. The 17 putative CAD homologues were designated *AtCAD1–AtCAD9* and *AtCAD101–AtCAD108* (see Tables 1 and 3). Each cDNA sequence was obtained from TAIR, and mRNA sequences from this study were deposited in GenBank.

Cloning and Heterologous Expression/Purification of *A. thaliana* CAD Homologues. For more information, see *Supporting Methods*.

Enzyme Characterization. Standard assays consisted of 1,3-bis[tris(hydroxymethyl)methylamino]propane (Bistris propane) buffer (100 mM, pH 6.25/100 μ l)/130 μ l (2–90 μ g) of purified CAD in Tris·HCl (20 mM, pH 7.5)/0.4 mM aldehyde 1–5/0.4 mM NADPH, in a total volume of 250 μ l. Enzymatic reactions were initiated by enzyme addition and, after 4 min incubation at 30°C, were stopped by adding glacial acetic acid (10 μ l); cinnamic acid (6.25 μ M, 10 μ l) was added as internal standard. An aliquot (80 μ l) of each assay mixture was subjected to reversed-phase HPLC analysis with liquid chromatography-MS and UV detection for product identification (data not shown; see *Supporting Methods*). Assays with individual substrates were performed in triplicate or tetraplicate, with controls in the absence of NADPH.

Optimum pH and temperature were individually determined for each CAD homologue and each aldehyde 1–5 by using standard assay conditions. For pH optima, incubations were carried out at 30°C with Mes buffer (100 mM, pH 5.1–6.8) or Bistris propane buffer (100 mM, pH 6.2–8.0); for temperature optima, incubations were performed at pH 6.25, but with various temperatures (20–50°C). Initial velocity kinetics were determined by individually assaying CAD1–CAD9 under standard conditions at pH 6.25 with 15 different aldehyde 1–5 concentrations (76–400 μ M) and at 30°C for 4 min (or 2 min for AtCAD5). Assays were also individually performed by using [4R-³H]NADPH or [4S-³H]NADPH (0.4 mM, 4.5 kBq; ref. 21), respectively, and were analyzed for radiochemical incorporation through stereospecific [³H] transfer into monolignols 6–10 (see Table 4, which is published as supporting information on the PNAS web site).

Knockout Mutants. Insertion mutant information was obtained from the SIGnAL web site, which can be accessed at <http://signal.salk.edu> (22). After searching the TAIR database, all available T-DNA insertion lines (T₃ seeds) of interest were ordered from the *Arabidopsis* Biological Resource Center (ABRC) at Ohio State University (Columbus, OH): SALK_019355 and SALK_040062 (AtCAD5), and SALK_030496 (AtCAD6) and SALK_037853 (AtCAD9). Homozygous plant lines were obtained as follows: Total genomic DNA was first isolated by using a REDExtract-N-AMP plant PCR kit according to the manufacturer's instructions. Left and right gene-specific primers, LP and RP (Table 5, which is published as supporting information on the PNAS web site), were then designed for each CAD gene of interest, as described at the SIGnAL website. Two sets of PCRs were carried out by using the touch-down method (ref. 23; see *Supporting Methods*): the first with LP and RP primers specific for each gene, as well as with the T-DNA left border primer (LBb1, 5'-GCGTGGACCGCTTGCT-GCAACT-3') and the second with LP and RP primers only. Homozygous lines were verified by the presence of single bands (\approx 500 base pairs), which were individually cloned into a pCR4-TOPO vector and sequenced to confirm the T-DNA insertion.

Results and Discussion

***Arabidopsis* Genome Analysis and Reclassification of Putative CAD Homologues.** The first gene purportedly encoding a CAD was reported in 1988 from bean (*Phaseolus vulgaris*; ref. 6). However, it actually encoded malic enzyme (24, 25), being misidentified in part because of no biochemical confirmation. Other research groups used the malic enzyme cDNA in the mistaken belief that it encoded CAD, such as to study monolignol pathway induction in the rubber tree (*Hevea brasiliensis*; ref. 26); others still refer to malic enzyme cDNA as encoding CAD (10). The first bona fide CAD gene was reported in 1992 (27) from tobacco (*Nicotiana tabacum*) stems, with another obtained in 1994 from loblolly pine (*Pinus taeda*; GenBank accession no. Z37992).

The TAIR database has 17 genes annotated as CAD-like (Tables 1 and 3). In the present study (Figs. 8 and 9, which are published as supporting information on the PNAS web site), the corresponding amino acid sequences for each were aligned against those of both bona fide tobacco (27) and loblolly pine (28) CADs, as well as to a putative CAD and a claimed SAD from aspen (20).

Nine of the 17 putative CADs had relatively high levels of similarity (57.1–82.9% and 61.0–76.5%) and identity (46.0–76.5% and 47.5–65.8%) to both *N. tabacum* and *P. taeda* CADs (Table 1), as well as to the putative aspen CAD (\approx 55–83%) and to the claimed aspen SAD (\approx 59–78%). Of those nine CADs, AtCAD6–8 had highest similarity (\approx 78%) and identity (68.5–72.1%) to the claimed aspen SAD. By contrast, the remaining eight (Table 3) shared essentially no homology to either *N. tabacum* or *P. taeda* CADs (0.9–1.6% similarity).

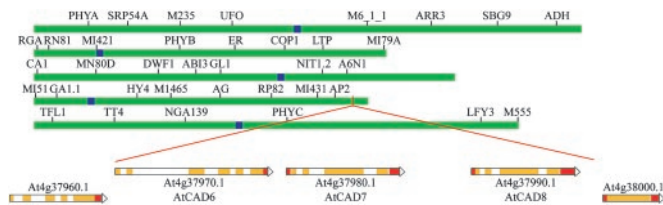


Fig. 2. Position of AtCAD6–AtCAD8 on chromosome 4 of *A. thaliana*.

Only AtCAD1–AtCAD9 with highest homology to bona fide CADs were chosen for detailed study (see Table 1 and Fig. 8). Relative to tobacco CAD, all had the highly conserved Zn1 catalytic center (C47, H69, and C163), the Zn-binding signature GHXXGXXXXXXGXXV, the Zn2 structural motif (C100, C103, C106, and C114), and the NADPH-binding domain [GLG-GV(L)G] motif (so-called Rossmann fold; refs. 4 and 29). Based on homology (18), AtCAD1–9 could be subclassified into two subgroups, with AtCAD5 and AtCAD4 (74% to ≈83% similarity) being most homologous to the bona fide *P. taeda*/*N. tabacum* CAD genes; the remaining seven were CAD-like but, of significantly lower homology (57.1–65.5% similarity).

The other eight annotated *Arabidopsis* CADs [including SAG 26 (11)], had essentially no homology to either tobacco or loblolly pine CADs (see Table 3 and Fig. 9), an observation requiring explanation. In *Arabidopsis*, SAG 26 annotation with a CAD function was based solely on a 67% similarity/56% identity to an apple (*Malus domestica*) cDNA claimed to encode a CAD (10), but whose function was actually unknown. Furthermore, whereas gene expression of SAG 26 was considered tightly correlated with senescence onset, as well as being defense-inducible (salicylic acid; ref. 11), there was again no biochemical context established.

Annotation of the eight *Arabidopsis* genes as being CADs was instead based on a relative degree of homology (82.5–49.8% similarity, see Table 3) to an alcohol dehydrogenase from *Eucalyptus gunnii* (30), whose precise physiological/biochemical function was actually unknown. The latter was CAD-annotated, even though the corresponding protein had very broad substrate specificity for a variety of aromatic substrates (30). Furthermore, both this gene, and the eight other annotated CADs, encode proteins lacking both the Zn catalytic center and the Zn-binding signature found in bona fide CAD (Fig. 9). It was thus concluded that this CAD annotation was misleading and, accordingly, the eight *Arabidopsis* genes were not considered further.

Chromosomal Organization and Cloning. *AtCAD1–9* genes are distributed in four of five *Arabidopsis* chromosomes: chromosome 1 (*AtCAD1*), chromosome 2 (*AtCAD2* and 3), chromosome 3 (*AtCAD4*), and chromosome 4 (*AtCAD5–9*), with *AtCAD6–8* genes being clustered together (Fig. 2), the significance of which is as yet unknown but potentially most interesting in terms of a defense response (discussed below).

Gene-specific primer sets (Table 6, which is published as supporting information on the PNAS web site) were next designed for each cDNA sequence, these being individually used in PCR amplifications to isolate target genes. To achieve this end, *Arabidopsis* total RNA was initially isolated from aerial tissues of 41-day-old plants, and by using this as a template, first-strand cDNA was synthesized. PCR amplification by using the touch-down method (23) was then individually performed with first-strand cDNA template, with this method ultimately giving seven of the nine target CAD-like genes (*AtCAD1* and *AtCAD4–9*). *AtCAD2* and *AtCAD3* genes were also obtained as above, but with total RNA isolated from 26-day-old plants.

CAD Recombinant Protein Expression and Kinetic Characterization. Crude protein extracts for each CAD homologue (see *Supporting Methods*) were prepared from cell pellets (derived from 250 ml of

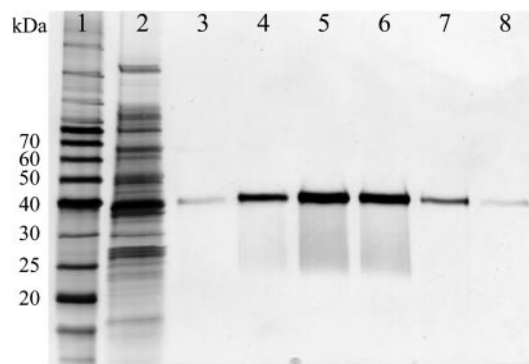


Fig. 3. Representative purification of CAD, using AtCAD5 for illustrative purposes. Lanes: 1, molecular mass ladder; 2, *Escherichia coli* crude extract; 3–8, fractions eluted from the metal chelate affinity column between 70 and 230 mM imidazole in Tris-HCl buffer contained pure AtCAD5. Proteins were visualized by silver staining.

culture medium) with, in most cases, ≈150 mg of total protein obtained. Each CAD was individually purified to apparent homogeneity (evaluated by SDS/PAGE with silver staining) after metal chelate affinity column chromatography, with each C-terminal His₆-tagged target protein individually eluted between 70 and 230 mM imidazole in Tris-HCl buffer. Fractions were analyzed by SDS/PAGE and those containing the target protein were combined, concentrated, and dialyzed. Typically, ≈2.0 mg of each pure protein was obtained (see Fig. 3, with AtCAD5 as an example). Purified proteins were directly used for enzyme characterization, with those catalytically active being stable up to 5 days at 4°C.

Enzyme assays and kinetic measurements were carried out by using all possible substrates 1–5 and products 6–10, in the presence of NADPH (100 μmol), with enzyme activities verified by HPLC analyses with both UV and electron impact MS detection (21, 31–33). [Syntheses of substrates 1–5 and products 6–10 were based on our previous strategies for both monolignols and lignans (see *Supporting Methods* and Scheme 1, which is published as supporting information on the PNAS web site).] Of the CAD homologues, AtCAD2–5, 7, and 8 were biochemically competent to reduce phenylpropenaldehyde substrates 1–5, with pH and temperature optima of ≈6.25 and 30–40°C, respectively, for each substrate (see Table 4). On the other hand, AtCAD1, 6, and 9 were of very low catalytic activity and only at high protein levels (≈140 μg); i.e., 0.031–0.224, 0.037–0.078, and 0–0.062 pKat per μg of protein, respectively. Furthermore, in an attempt to establish whether low catalytic activity was somehow due to attachment of the C-terminal His tag, N-terminal His-tagged protein (AtCAD1) was also studied. However, this variation had no measurable effect on either substrate versatility or on catalytic efficacy relative to the C-terminal His-tagged analogue. Indeed, because the isoforms (AtCAD1, 6, and 9) were also of the lowest homology relative to AtCAD4 and 5, their low catalytic activity was therefore not unexpected (see Table 1). All of the catalytically active CAD homologues were, however, type A dehydrogenases; i.e., abstracting the pro-R [³H]hydride from [4R-³H]NADPH, but not the corresponding [³H]hydride from [4S-³H]NADPH (ref. 21 and Table 4), which is in agreement with earlier studies by using CAD from *Forsythia suspensa* (2).

AtCAD5 and AtCAD4 were the most catalytically active overall (see Table 2), with *p*-coumaryl aldehyde (1) being the preferred substrate for both enzymes. AtCAD5 also effectively used sinapyl (5), coniferyl (3), and 5-hydroxyconiferyl (4) aldehydes, as well to a lesser extent, caffeyl aldehyde (2) (see Figs. 4 and 5), in accordance with the relatively broad substrate versatility of this enzyme class. AtCAD4 also quite readily used substrates 2–4, whereas

Table 2. Kinetic parameters for CAD homologues AtCAD2–5, 7, and 8

	Substrate	K_m , μM	V_{max} , $\mu\text{Kat}/\mu\text{g}$	k_{cat} , sec^{-1}	k_{enz} , $\text{M}^{-1}\cdot\text{sec}^{-1}$
AtCAD4	1	47	44.0	3.44	74,000
	2	87	17.1	1.33	15,000
	3	65	26.8	2.10	32,000
	4	85	32.3	2.52	30,000
	5	274	9.2	0.72	2,600
AtCAD5	1	13	187.3	14.52	1,091,000
	2	68	94.1	7.30	107,000
	3	35	157.4	12.19	348,000
	4	22	106.9	8.28	370,000
	5	20	177.0	13.72	700,000
AtCAD2	1	114	3.3	0.27	2,400
	2	161	22.2	1.81	11,000
	3	452	8.0	0.65	1,400
	4	336	16.4	1.34	4,000
	5	2,161	48.1	3.93	1,800
AtCAD3	1	292	20.1	1.65	5,600
	2	581	9.7	0.80	1,400
	3	362	4.8	0.39	1,100
	4	534	17.9	1.47	2,800
	5	629	9.1	0.74	1,200
AtCAD7	1	320	28.6	2.18	6,800
	2	3,685	79.0	6.04	1,600
	3	675	13.0	0.99	1,500
	4	756	2.7	0.21	280
	5	313	0.6	0.05	150
AtCAD8	1	302	20.4	1.59	5,300
	2	683	7.0	0.54	800
	3	141	5.6	0.44	3,100
	4	457	10.4	0.81	1,800
	5	898	28.9	2.25	2,500

sinapyl aldehyde (5) was, by comparison, a poor substrate; i.e., indicative of a somewhat more restricted substrate specificity.

However, AtCAD5 and AtCAD4 differed substantially in their

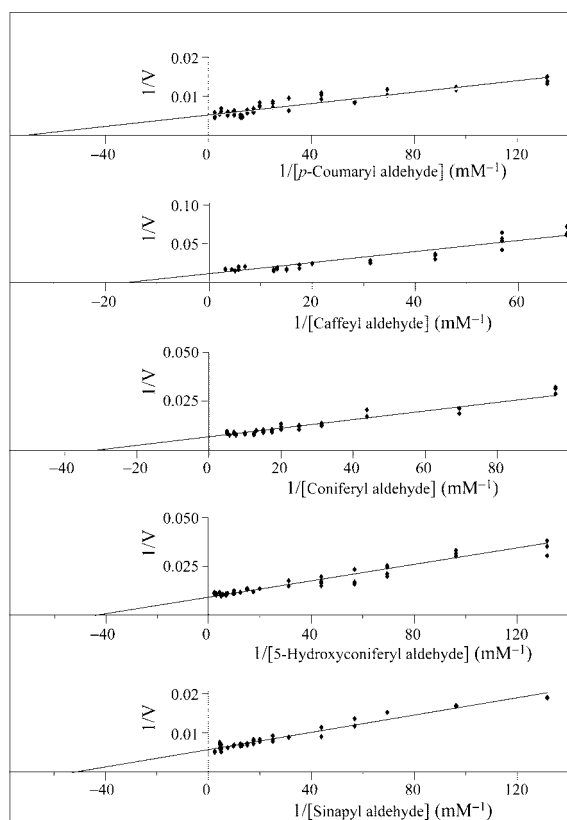


Fig. 4. Lineweaver–Burk plots of AtCAD5 for substrates 1–5.

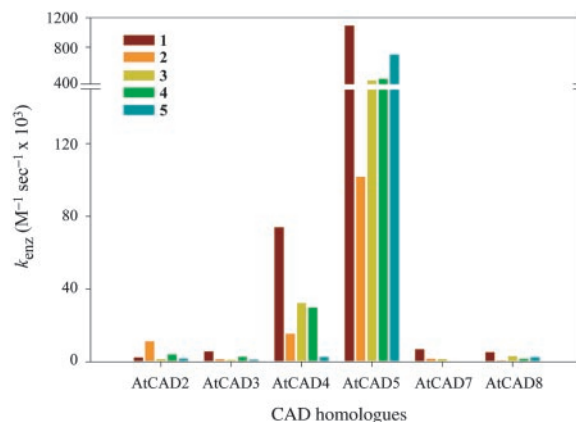


Fig. 5. Relative substrate 1–5 efficacy of *Arabidopsis* recombinant CAD homologues.

overall catalytic properties, as revealed by k_{enz} values (calculated by dividing K_{cat} by K_m): with substrates 1–5, AtCAD5 was more effective than AtCAD4 by factors of 15, 7, 11, 12, and 270 times, respectively (i.e., differences of ≈ 1 to 2 orders of magnitude; Table 2). For *p*-coumaryl aldehyde (1), coniferyl aldehyde (3) and 5-hydroxyconiferyl aldehyde (4), these differences can be explained on the basis of both binding (K_m values increasing ≈ 2 - to 4-fold with AtCAD4) and lower turnover numbers (k_{cat} decreases ≈ 3 - to 6-fold with AtCAD4). Differences in k_{enz} for caffeoyl aldehyde (2), on the other hand, resulted from a small decrease in K_m and a substantial increase in k_{cat} between AtCAD5 and AtCAD4. The most profound difference between AtCAD5 and AtCAD4, however, occurred with sinapyl aldehyde (5), with a >10 -fold increase in K_m and a ≈ 20 -fold increase in k_{cat} . Based on the substrate versatility preference of AtCAD4 for *p*-coumaryl (1), coniferyl (3), and sinapyl (5) aldehydes, this isoform thus displays quite similar characteristics to that of a partially purified gymnosperm CAD from spruce (34), in as far as the latter also poorly used sinapyl aldehyde (5).

Arabidopsis AtCAD5 is also catalytically more active for sinapyl aldehyde (5) than the purported aspen SAD, claimed solely responsible for syringyl lignin formation (20). However, subsequent reanalysis (3) of the kinetic data for the claimed sinapyl aldehyde (5) specific SAD revealed that the claims were unfounded, because the so-called SAD could reduce each of the substrates 1–5. Indeed, overall it was actually catalytically more active for substrates 1–5 than a putative CAD isoform, which was also present in aspen (summarized in 3). Clearly, with catalytic properties of both *Arabidopsis* AtCAD4 and AtCAD5 as determined, there is no need to implicate a distinct SAD for specific generation of sinapyl alcohol 10 in angiosperms, including *Arabidopsis*.

By contrast, the AtCAD1–3 and 6–9 homologues were catalytically less active, with K_m values for potential substrates 1–5 typically higher (relative to AtCAD5) and overall turnover numbers (k_{cat}) lower by at least one order of magnitude, respectively. AtCAD2, however, used caffeoyl aldehyde (2) most effectively as a substrate, whereas AtCAD3 had a slight preference for *p*-coumaryl (1) and 5-hydroxyconiferyl (4) aldehydes. On the other hand, AtCAD7 and 8 both used *p*-coumaryl aldehyde (1) as the best substrate, albeit only somewhat better than other potential substrates. Whereas AtCAD6–8 have the highest homology ($\approx 78\%$ similarity) to the claimed aspen SAD in aspen, neither AtCAD7 nor 8 displayed any substrate preference for sinapyl aldehyde (5). Thus, there is no biochemical data, for any of the CAD homologues, supporting the notion of a specific SAD isoform; i.e., in terms of binding, turnover, substrate preferences, etc.

It is also important to note that whereas AtCAD2, 3, 7, and 8 display more moderate levels of CAD activities (relative to

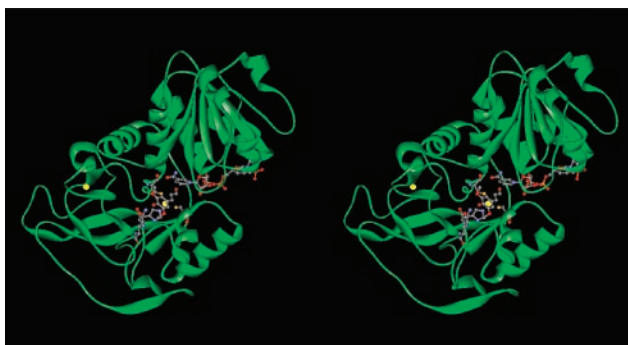


Fig. 6. A stereoview showing the distribution of structural elements of AtCAD4. The two Zn atoms are shown in yellow together with three coordinating amino acids (C47, H69, and C163), Q130, NADP(H), and sinapyl aldehyde (5). This figure was prepared by using WEB VIEWER.

AtCAD5/AtCAD4), none of their physiological functions are unambiguously established to this point. Gene expression profiles suggested previously indicated that AtCAD7 was inducible in response to *Pseudomonas syringae* infection, perhaps suggesting an alternative metabolic role in plant defense (7); indeed, another study (35) indicated that AtCAD7 (Eli-3) may be an aromatic alcohol dehydrogenase of broad substrate specificity. (However, no characterization of ELI-3 with purified recombinant protein was carried out.)

Molecular Modeling of AtCAD4 and AtCAD5. With the marked differences in substrate preferences of AtCAD5 and AtCAD4 regarding sinapyl aldehyde (5), a molecular modeling study was conducted to provisionally explain such profound differences. A BLASTP search of the Protein Data Bank (PDB) database revealed that AtCAD4 and AtCAD5 had highest sequence similarities (58.3% and 59.1% respectively) to that of the *Sulfolobus solfataricus* NAD-dependent alcohol dehydrogenase, whose crystal structure is established (1JVB; ref. 36). Positions of the second structural elements in its crystal structure also matched well with the predicted positions for those elements in AtCAD4 and AtCAD5, based on PSPRED, which can be accessed at <http://bioinf.cs.ucl.ac.uk/psipred> and PHD, which can be accessed at <http://npsa-pbil.ibcp.fr>.

Amino acid substitutions, insertions, and deletions were next performed by using the graphics program O (37), starting from the *S. solfataricus* alcohol dehydrogenase coordinates (PDB ID code 1JVB), followed by quick-energy minimization by using X-PLOR (38) with potential function parameters of CHARMM19 as described (39). The initial positions of substrates and NADPH were obtained through the solid docking module on QUANTA (BioSYM/Micron Separations), which is based on conformational space, followed by a quick energy minimization by X-PLOR (38).

The backbones of AtCAD4- and AtCAD5-modeled structures did not change significantly (Fig. 6) and clearly showed properly sized binding pockets for NADPH and the cinnamyl aldehyde substrate near the catalytic zinc site made of C47, H69, and C163 (see Fig. 8, with AtCAD4 as example). In this modeled structure, the two methoxyl groups of sinapyl aldehyde (5) can fit snugly into the hydrophobic environment of both AtCAD5- and AtCAD4-active sites. Significantly, all residues within contact or potentially interacting distances to the substrate are conserved between AtCAD4 and AtCAD5, except for residue 129/130 (Gln and Lys in AtCAD5 and AtCAD4, respectively). A provisional explanation is that these residues help account for differences in overall catalytic behavior, because the side-chain amide group of Gln is capable of both donating and accepting hydrogen atoms through H-bonding to the phenolic hydroxyl group of 5, whereas the primary amine group in the Lys residue, ionizable at neutral pH, can withdraw electrons. However, a possible indirect contribution of residue 127/128, which

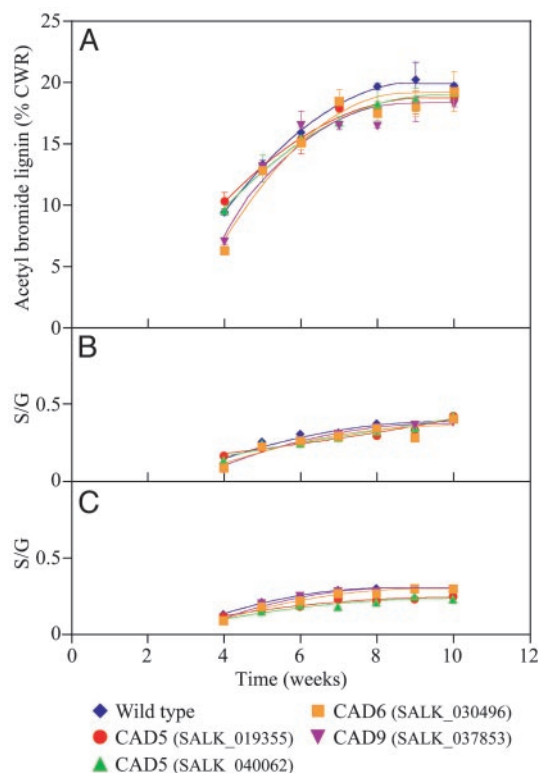


Fig. 7. Time course of *Arabidopsis* (Columbia) growth and development versus lignin content/monomer composition ratios. (A) Acetyl bromide lignin contents. (B) S:G ratios by nitrobenzene oxidation. (C) S:G ratios by thioacidolysis. CWR, cell wall residue.

are Asn and Asp in AtCAD5 and AtCAD4, respectively, cannot be ruled out, even though it is apparently not within an interacting distance to the substrate. Both residues (128 and 130 in AtCAD4 and 127 and 129 in AtCAD5) are located immediately after the major insertion of ¹²¹SYNDVY¹²⁶, as compared with the *S. solfataricus* alcohol dehydrogenase. Therefore, due to this uncertainty, the exact distances between the substrate and those two residues cannot be estimated from this modeling study.

Identifying CAD Metabolic Networks Through Mutant Analysis. With four knockout lines for AtCAD5, AtCAD6, and AtCAD9 available from ABRC (see Table 5 for transgene orientations), we investigated whether any would affect either lignin deposition and/or lignin monomer composition, or whether various CAD metabolic networks were present thus conferring functional redundancy.

Comparative analyses of both mutant and wild-type *Arabidopsis* plants were therefore next carried out from germination to maturation, with sampling at regular points in the life cycle. By contrast, studies of various mutant *Arabidopsis* lines, including effects on lignin deposition (13, 40), have long been compromised by lack of such detailed analyses, and, surprisingly, typically monitor only one time point (harvesting; ref. 13). Accordingly, such studies often ignore the effects of, for example, phenotypical changes in growth/development rates and differential rates of lignin deposition per cell wall maturation (3). Plants were thus harvested at weekly intervals (from 4 to 10 weeks) for both wild type and knockouts, with bolting stems extracted (see *Supporting Methods*) and subjected to estimations of total lignin contents and monomer compositions. The acetyl bromide lignin method (see *Supporting Methods*) was chosen over Klason lignin analysis, because the latter frequently gives overestimations of lignin contents (>26–40% of cell wall residue) with *Arabidopsis* due to contaminating non-lignin components

(data not shown and ref. 3). Monomer compositions were estimated by using both nitrobenzene oxidation (not specific to monolignol moieties in lignin) and thioacidolysis (presumed specific to 8-*O*-aryl-linked moieties in lignin). However, these methods only give a crude estimate of syringyl:guaiacyl (S:G) ratios, because they typically only account for ≈20–30% of the estimated lignin present (3) and, in some instances, even less (13).

The acetyl bromide lignin analyses of *Arabidopsis* wild-type and CAD knockout homozygous lines indicated a small level of variability in lignin deposition throughout growth and development; however, at maturity (≈10 weeks), the maximum values were more or less equivalent to that of wild-type plants (Fig. 7A). AtCAD6 and AtCAD9 initially showed very slight decreases in lignin deposition, but the variability was quite minor and not significantly different at plant maturation, nor did the AtCAD5 mutant lines differ significantly from wild-type plants by maturation. Estimations of S:G ratios, by using both nitrobenzene oxidation (Fig. 7B) and thioacidolysis (Fig. 7C) analyses, also revealed some small differences in the S:G ratios during early stages of growth and development, but, which at maturation was largely insignificant, except for a very small decrease in the releasable S component by thioacidolysis; however, it is noteworthy that the S levels increased slowly but steadily up to the maturation point, again being quite similar to wild type at this developmental stage.

Thus, based on these data, *AtCAD5* gene disruption apparently results only in slightly delayed syringyl lignin deposition during early phases of growth/development in the various cell types (xylem and interfascicular fibers) and, hence, presumably reflects decreased rates of cell wall maturation. However, syringyl lignin deposition is never “knocked out,” despite this isoform being the most catalytically active for sinapyl aldehyde (5). Indeed, these data reveal that by maturation, the presence of the other CAD homologues eventually permits lignin formation to essentially fully occur (including reaching the wild-type S:G ratios).

Taken together, these data provide support for CAD multigene networks ensuring that monolignols **6**, **8**, and **10** are formed, even if, for example, expression of one gene (such as *AtCAD5*) is disrupted and the syringyl lignin deposition rate is slightly delayed. Whether the genes in the proposed networks in the knockouts are

expressed similarly as for wild-type plants, or differentially to compensate, remains to be determined.

Surprisingly, CAD is often reported to have a rate-limiting (regulatory) capacity during monolignol biosynthesis (19), which is an enigmatic assertion given that it is the final step in monolignol **6**, **8**, and **10** formation. Furthermore, Fell's (41) definition of rate-limiting (regulatory) steps as “fractional change in metabolic flux effected by a fractional change in amount (or activity) of the enzyme” does not support this notion. Indeed, we previously established (28), by detailed metabolic flux/transcriptional regulation studies, and comprehensive reevaluation of data obtained from various transgenic (CAD-down-regulated) plant lines (3), that CAD unequivocally does not have a key (rate-limiting) capacity relative to other steps in terms of carbon allocation. This finding is again demonstrated in this study. That is, even under conditions of a single gene disruption, which potentially could have become a rate-limiting step in the S-monolignol forming pathway, other isoforms were capable of compensating, i.e., to ensure that sinapyl alcohol (**10**) formation could essentially still occur.

In summary, based on the findings of this study, it is tempting to speculate that *AtCAD4* is mainly used in *p*-coumaryl (**6**) and coniferyl (**8**) alcohol formation, whereas *AtCAD5* can be used to normally generate all three monolignols [i.e., including sinapyl alcohol (**10**)]. Indeed, the lignin in interfascicular fibers in *Arabidopsis* is generally considered to have a larger sinapyl alcohol (**10**)-derived content than xylem cells, perhaps suggesting dominant expression of *AtCAD5* in these cells (42). However, β -glucuronidase-promoter expression analysis for each of the CAD homologues revealed a complex pattern of expression, including significant expressional overlap both temporally and spatially during *Arabidopsis* growth and development (e.g., *AtCAD4* and *AtCAD5*) (S.-J. K., H. W. Kim, L. B. Davin, V. R. Franceschi, and L. N. G., unpublished data). In this way, the organism ensures that lignin deposition occurs, even in the case of disruption of *AtCAD5*, again reflecting the exquisite control of lignin assembly.

This work was supported in part by National Science Foundation *Arabidopsis* 2010 Project Grant MCB-0117260, Department of Energy Grant DE-FG03-97ER20259, National Aeronautics and Space Administration Grant NAG 2-1198, and the G. Thomas and Anita Hargrove Center for Plant Genomic Research.

- Gross, G. G., Stöckigt, J., Mansell, R. L. & Zenk, M. H. (1973) *FEBS Lett.* **31**, 283–286.
- Mansell, R. L., Gross, G. G., Stöckigt, J., Franke, H. & Zenk, M. H. (1974) *Phytochemistry* **13**, 2427–2435.
- Anterola, A. M. & Lewis, N. G. (2002) *Phytochemistry* **61**, 221–294.
- Lewis, N. G., Davin, L. B. & Sarkanen, S. (1999) in *Comprehensive Natural Products Chemistry*, eds. Barton, D. H. R., Nakanishi, K. & Meth-Cohn, O. (Elsevier, London), Vol. 3, pp. 617–745.
- Lewis, N. G. & Davin, L. B. (1999) in *Comprehensive Natural Products Chemistry*, eds. Barton, D. H. R., Nakanishi, K. & Meth-Cohn, O. (Elsevier, London), Vol. 1, pp. 639–712.
- Walter, M. H., Grima-Pettenati, J., Grand, C., Boudet, A. M. & Lamb, C. J. (1988) *Proc. Natl. Acad. Sci., USA* **85**, 5546–5550.
- Kiedrowski, S., Kawalleck, P., Hahlbrock, K., Somssich, I. E. & Dangel, J. L. (1992) *EMBO J.* **11**, 4677–4684.
- Somers, D. A., Nourse, J. P., Manners, J. M., Abrahams, S. & Watson, J. M. (1995) *Plant Physiol.* **108**, 1309–1310.
- Baucher, M., Van Doorselaere, J., Gielen, J., Van Montagu, M., Inzé, D. & Boerjan, W. (1995) *Plant Physiol.* **107**, 285–286.
- Kim, S.-H., Lee, J.-R., Shin, Y.-U., An, G. & Kim, S.-R. (1999) *J. Microbiol. Biotechnol.* **9**, 475–481.
- Quirino, B. F., Normanly, J. & Amasino, R. M. (1999) *Plant Mol. Biol.* **40**, 267–278.
- Tavares, R., Aubourg, S., Lecharny, A. & Kreis, M. (2000) *Plant Mol. Biol.* **42**, 703–717.
- Sibout, R., Eudes, A., Pollet, B., Goujon, T., Mila, I., Granier, F., Séguin, A., Lapiere, C. & Jouanin, L. (2003) *Plant Physiol.* **132**, 848–860.
- The *Arabidopsis* Genome Initiative (2000) *Nature* **408**, 796–815.
- Lewis, N. G., Davin, L. B. & Franceschi, V. (2002) in *Plant Physiol.*, ed. Ausubel, F. M. (American Society of Plant Biologists, Rockville, MD), Vol. 129, pp. 394–437.
- Kim, S.-J., Bedgar, D. L., Moinuddin, S. G., Kim, M.-R., Cardenas, C., Davin, L. B. & Lewis, N. G. (2003) *14th International Conference on Arabidopsis Research* (Univ. of Wisconsin, Madison, WI), p. 179.
- Anterola, A. M., Chung, B.-Y., Kim, S.-J., Bedgar, D. L., Davin, L. B. & Lewis, N. G. (2003) *First International Meeting on Phytochemistry and Biology of Lignans, Bornheim-Walberberg, Germany, Phytochemical Society of Europe* (Kluwer, Dordrecht, The Netherlands), pp. 2–3.
- Costa, M. A., Collins, R. E., Anterola, A. M., Cochrane, F. C., Davin, L. B. & Lewis, N. G. (2003) *Phytochemistry* **64**, 1097–1112.
- Baucher, M., Chabbert, B., Pilate, G., Van Doorselaere, J., Tollier, M.-T., Petit-Conil, M., Cornu, D., Monties, B., Van Montagu, M., Inzé, D., et al. (1996) *Plant Physiol.* **112**, 1479–1490.
- Li, L., Cheng, X.-F., Leshkevich, J., Umezawa, T., Harding, S. A. & Chiang, V. L. (2001) *Plant Cell* **13**, 1567–1585.
- Dinkova-Kostova, A. T., Gang, D. R., Davin, L. B., Bedgar, D. L., Chu, A. & Lewis, N. G. (1996) *J. Biol. Chem.* **271**, 29473–29482.
- Alonso, J. M., Stepanova, A. N., Leisse, T. J., Kim, C. J., Chen, H., Shinn, P., Stevenson, D. K., Zimmerman, J., Barajas, P., Cheuk, R., et al. (2003) *Science* **301**, 653–657.
- Don, R. H., Cox, P. T., Wainwright, B. J., Baker, K. & Mattick, J. S. (1991) *Nucleic Acids Res.* **19**, 4008.
- Walter, M. H., Grima-Pettenati, J., Grand, C., Boudet, A. M. & Lamb, C. J. (1990) *Plant Mol. Biol.* **15**, 525–526.
- Walter, M. H., Grima-Pettenati, J. & Feuillet, C. (1994) *Eur. J. Biochem.* **224**, 999–1009.
- Kush, A., Goyvaerts, E., Chye, M.-L. & Chua, N.-H. (1990) *Proc. Natl. Acad. Sci. USA* **87**, 1787–1790.
- Knight, M. E., Halpin, C. & Schuch, W. (1992) *Plant Mol. Biol.* **19**, 793–801.
- Anterola, A. M., Jeon, J.-H., Davin, L. B. & Lewis, N. G. (2002) *J. Biol. Chem.* **277**, 18272–18280.
- Rossmann, M. G., Moras, D. & Olsen, K. W. (1974) *Nature* **250**, 194–199.
- Goffner, D., Van Doorselaere, J., Yahiaoui, N., Samaj, J., Grima-Pettenati, J. & Boudet, A. M. (1998) *Plant Mol. Biol.* **36**, 755–765.
- Katayama, T., Davin, L. B., Chu, A. & Lewis, N. G. (1993) *Phytochemistry* **33**, 581–591.
- Nose, M., Bernards, M. A., Furlan, M., Zajicek, J., Eberhardt, T. L. & Lewis, N. G. (1995) *Phytochemistry* **39**, 71–79.
- Anterola, A. M., van Resnburg, H., van Heerden, P. S., Davin, L. B. & Lewis, N. G. (1999) *Biochem. Biophys. Res. Commun.* **261**, 652–657.
- Lüderitz, T. & Grisebach, H. (1981) *Eur. J. Biochem.* **119**, 115–124.
- Somssich, I. E., Wernert, P., Kiedrowski, S. & Hahlbrock, K. (1996) *Proc. Natl. Acad. Sci. USA* **93**, 14199–14203.
- Esposito, L., Sica, F., Raia, C. A., Giordano, A., Rossi, M., Mazzarella, L. & Zagari, A. (2002) *J. Mol. Biol.* **318**, 463–477.
- Jones, T. A., Zou, J. Y., Cowan, S. W. & Kjeldgaard, M. (1991) *Acta Crystallogr. A* **47**, 110–119.
- Brunger, A. T. (1992) *X-PLOR*, a System for Crystallography and NMR (Yale Univ. Press., New Haven, CT), Version 3.1.
- Min, T., Kasahara, H., Bedgar, D. L., Youn, B., Lawrence, P. K., Gang, D. R., Halls, S. C., Park, Hilsenbeck, J. L., Davin, L. B., et al. (2003) *J. Biol. Chem.* **278**, 50714–50723.
- Jones, L., Ennos, A. R. & Turner, S. R. (2001) *Plant J.* **26**, 205–216.
- Fell, D. (1997) *Understanding the Control of Metabolism* (Portland Press, London).
- Meyer, K., Shirley, A. M., Cusumano, J. C., Bell-Lelong, D. A. & Chapple, C. (1998) *Proc. Natl. Acad. Sci. USA* **95**, 6619–6623.